MECHANIKA TEORETYCZNA
I STOSOWANA
Journal of Theoretical
and Applied Mechanics
4, 30, 1992

A SERIES SYSTEM THROWING A BATCH OF ELASTIC PROJECTILES FROM A TUBE LAUNCHER LOCKED BY A DIAPHRAGM

JÓZEF KROMKA

Military Airforce Technical Institute, Warsaw

Methods and results of examination of a multiprojectile tube launcher are presented. A linear displacement of succesive projectiles along the tube was defined and a pressure behind the pusher plate was measured. Complementary tests were necessary to describe completely the launch process during which the friction of the pusher plate and projectiles as well as the elasticity and the diaphragm rupture forces were found. The forces and pressures values measured were approximated to mathematical functions. The launch model throwing a batch of projectiles displaced under a pressure resulting from ejection charge was verified in a series of numerical calculations. Computed outlet velocities of the projectiles were compared with those obtained in experiments.

1. Introduction

Modern Armies and Air Forces are equipped with a lot of small-calibre cluster bombs (projectiles) that can be thrown from the tube launcher (cf [1,2]).

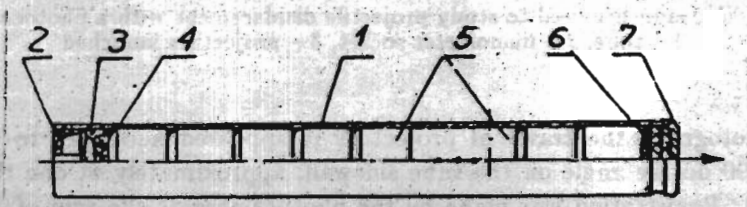

Fig. 1. Tube launcher; 1 – tube, 2 – tube bottom, 3 – ejection charge, 4 – pusher plate, 5 – projectile, 6 – tube packing, 7 – diaphragm

The projectiles in these launchers (Fig.1) are placed in series (5), i.e. arranged one after another, and thrown by an ejection cartridge (3) which is the source of pressure caused by a burning propellant charge. A pusher plate (4) moves under

this pressure shifting a batch of projectiles (5) in the outlet direction. During their movement clearances between them are eliminated, the tube packing (6) is squeezed and subsequently the diaphragm (7) attached to the tube (1) is ruptured.

The movement of a batch of pro jectiles has not been analyzed yet by any author. There is some kind of analogy to the movement of a train in the case when rail cars are pushed (cf [3,4]), however projectiles are not coupled like train coaches and the mass of the batch changes stepwise as the subsequent projectile leaves the tube. Investigations made in order to describe the ballistic model of a projectiles launch have been discussed in this paper.

2. Experiments

Two self-dependent methods were used to measure the displacement of projectiles inside the tube. They were accompanied by the simultaneous measurement of a pressure behind the pusher plate at the botton of the tube.

2.1. Registration of projectiles travel by a photocamera

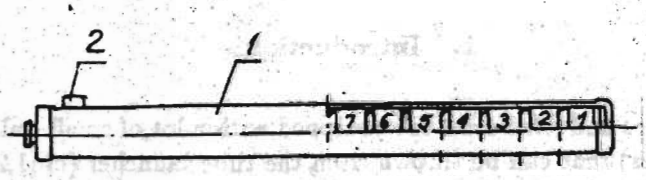

Fig. 2. Tube launcher used to study projectile displacement with a photocamera; 1 – tube, 2 – manometer socket, 3 – projectiles launched

To photograph the travel of projectiles it appeared necessary to cut out a sector of 90 degree angle on the tube sidewall, approximately at one third of its lenght (1). Registration was made by the photocamera at the rate of N frames per second. Photograph (Fig.3) shows one of the frames registered during the projectile launch. From the number of subsequent frames it was possible to find the distance travelled by the projectiles. By differentiating it with respect to time the velocity of projectiles has been found which is illustrated in Fig.4 ÷ 10. The pressure was measured conventionally at the spot where a manometer (2) was located, see Fig.2.

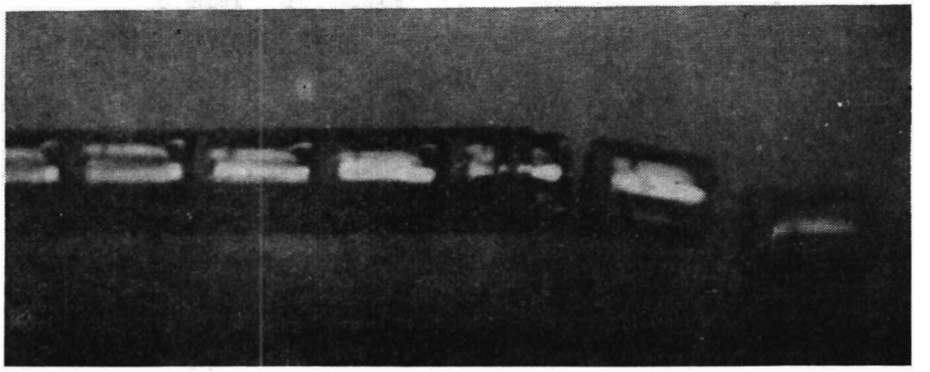

Fig. 3. Positioning of projectiles during launch ($t = 0.14$ s)

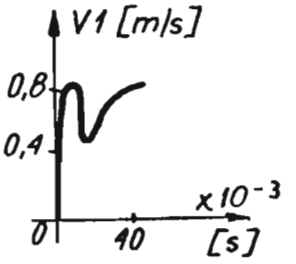

Fig. 4. Velocity of the 1st projectile versus time

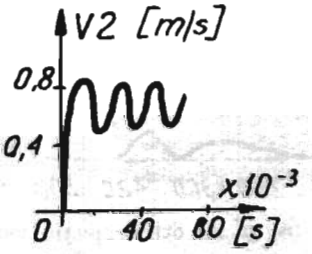

Fig. 5. Velocity of the 2nd projectile versus time

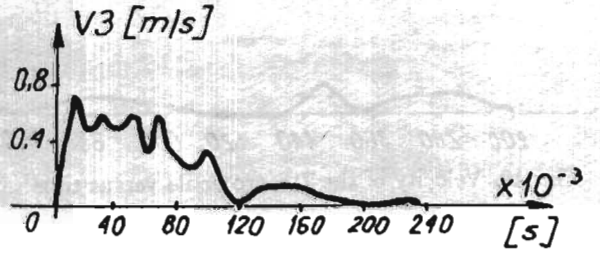

Fig. 6. Velocity of the 3rd projectile versus time

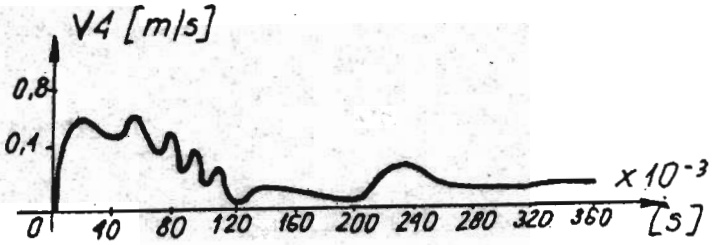

Fig. 7. Velocity of the 4th projectile versus time

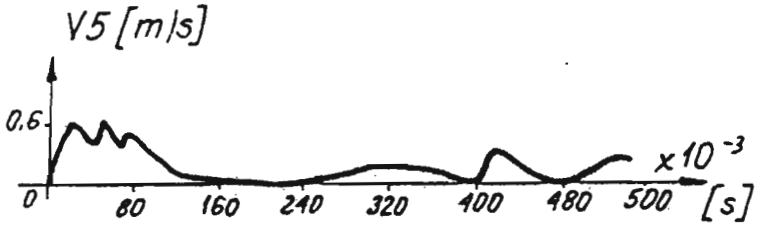

Fig. 8. Velocity of the 5th projectile versus time

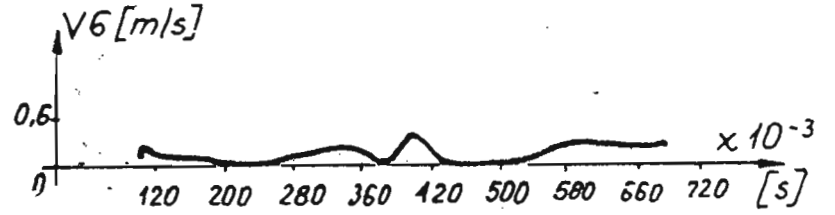

Fig. 9. Velocity of the 6th projectile versus time

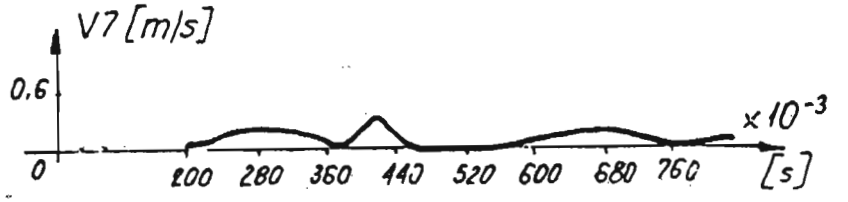

Fig. 10. Velocity of the 7th projectile versus time

2.2. Registration of projectiles travel by photoelectric sensors

The travel of projectiles inside the tube can also be monitored by a measuring system shown in Fig.11. Four photoelectric sensors $F1 \div F4$ closed in casings (2) were attached to the tube at even distances between them. Four light bulbs (3) were placed opposite to them on the other side of the tube. The bulbs $B1 \div B4$ were powered from their own power supply. The projectile lenght was assumed to be base for measurements. There were holes made right through the tube wall (1) in spaces between the projectiles so that the clearance Cl between the projectile elements (9,10) enabled the light to propagate from the bulbs to the photoelectric sensors $F1 \div F4$ (see Fig.11) and to be blanked off by travelling projectiles, respectively.

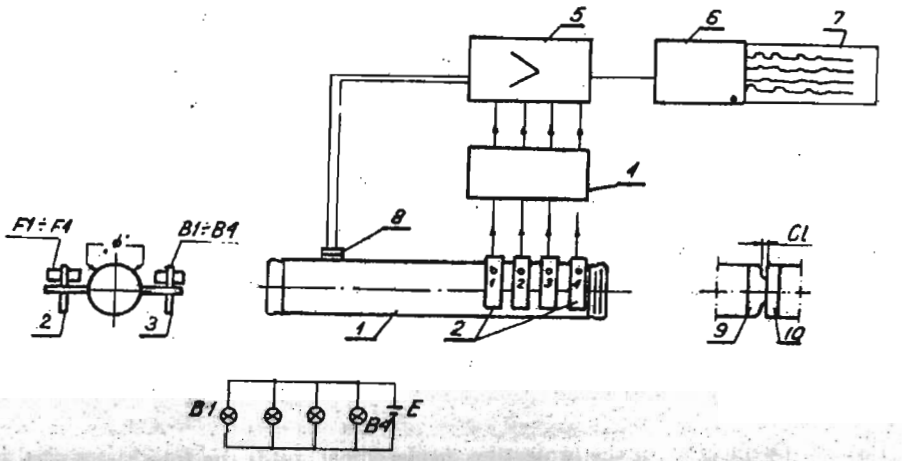

Fig. 11. Block diagram of projectile travel registration system with application of photoelectric sensors; 1 – tube, 2 – photoelectric sensors casings, 3 – bulbs casings, 4 – four channel amplifier, 5 – registrator amplifier, 6 – registrator, 7 – light–sensitive paper, 8 – manometer, 9 – elements of the projectiles (Cl – clearance)

The position of the measuring system before launch is such that light from the bulbs goes through the holes, i.e. between the projectiles and is detected by the photoelectric sensors. Photodiodes $D1 \div D4$ together with transistors $T5$ constitute the first stage of a four channel signal amplifier (4), (see Fig.11). Electric signal from the first diode is amplified by transistor $T1$ (see Fig.12) and goes through variable resistors $P1$ to amplifier (5) (see Fig.11) and finally comes to recorder (6). Signals from other sensors (2) travel in the same way. Variable resistors $P1 \div P4$ are used to set up the amplitude of electric signals. A piezoelectric manometer was placed into socket (8) (see Fig.11). Its electric signal is amplified (5) and registered by loop oscillograph (6). The projectiles shift

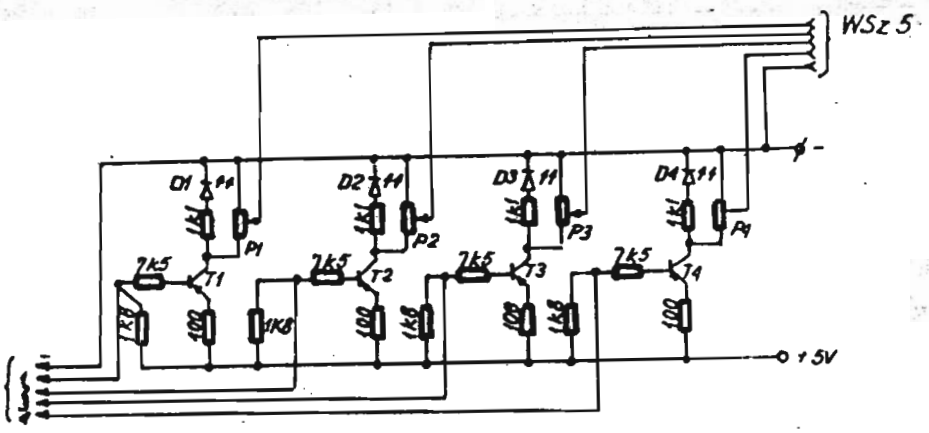

T1 ÷ T4 - BCAP 77
P1 ÷ P4 - DL 104 680 & 10% 0,5W
F1 ÷ F4 - BPY 22
T5 - BCA P0 7B

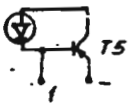

Fig. 12. Electric signal amplifier

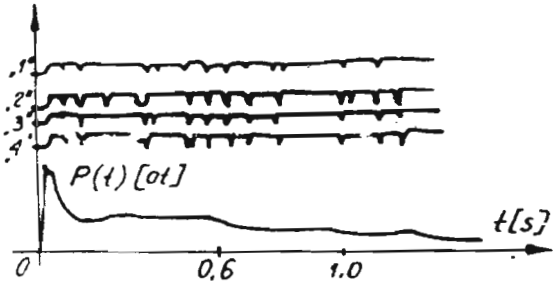

Fig. 13. Oscillogram of the projectiles displacement inside the tube aloug with the pressure curve; 1, 2. 3, 4 – diagrams of the consecutive projectiles displacements registered by photoelectric sensors, 5 – diagram of pressure versus launch time

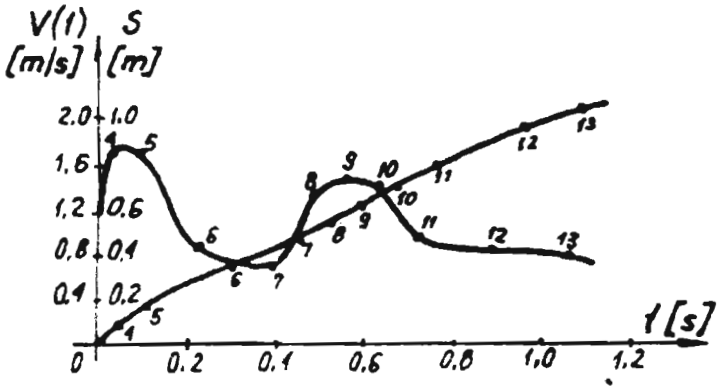

Fig. 14. Distances travelled and velocities of the projectiles registered by sensor No.1; 1 – velocity, 2 – distance

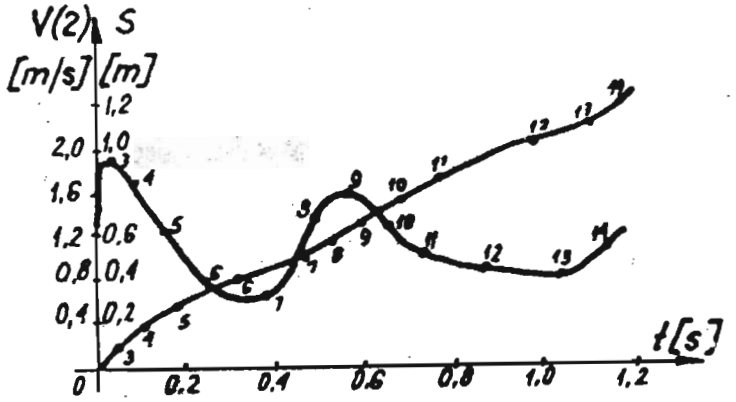

Fig. 15. Distances travelled and velocities of the projectiles registered by sensor No.2;
1 – velocity, 2 – distance

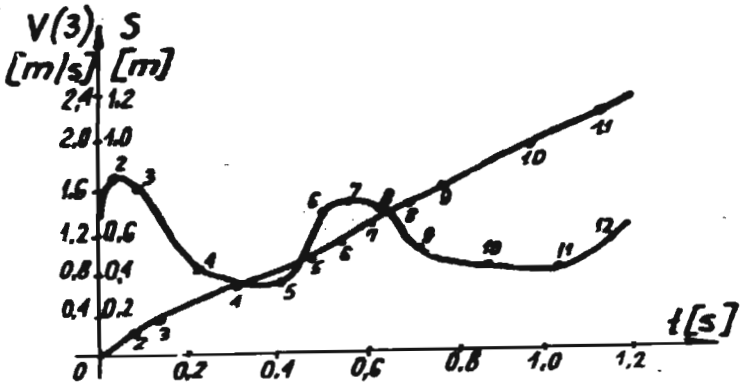

Fig. 16. Distances travelled and velocities of the projectiles registered by sensor No.3;
1 – velocity, 2 – distance

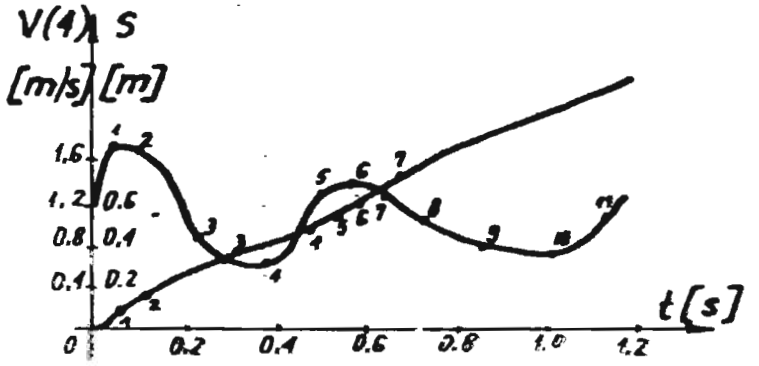

Fig. 17. Distances travelled and velocities of the projectiles registered by sensor No.4;
1 – velocity, 2 – distance

interrupts the seams of light between electric bulbs and photoelectric sensors. The resulting modulation of electric signals coming from these sensors is registered on a light-sensitive paper. Fig.13 shows these signals and the pressure measured by the piezoelectric manometer registered during the projectiles travel. From this photograph it is possible to find the velocities of travelling projectiles. The velocity envelopes taken from subsequent sensors (see Fig.14 ÷ 17) show the variation of the projectile velocity of travel.

2.3. Complementary studies

As a complement to ballistic tests the stationary studies have been made to find particular characteristics of launcher assemblies. The diaphragm rupture force was measured (see Fig.18), as well as pusher plate friction force (Fig.19) and elasticity forces of the projectile (Fig.20).

The pressure measurement results (see Fig.13) were approximated stepwise by polynomials of 4th and 5th order, respectively and by the straight line (Eq (2.1)).

The diaphragm rupture force (Fig.18) and pusher plate friction force were approximated by a polynomial of 4th order with various coefficients (Eqs (2.2) and (2.3)).

The elasticity force of projectiles was approximated by the function (Eq (2.4))

— for the time interval $t_0 - t_1$

$$p(t) = A(5)t^5 + A(4)t^4 + A(3)t^3 + A(2)t^2 + A(1)t + A(0)$$

— for time interval $t_1 - t_2$

$$p(t) = B(4)t^4 + B(3)t^3 + B(2)t^2 + B(1)t + B(0)$$

— for time interval $t_2 - t_k$

$$p(t) = C(1)t + C(0) \tag{2.1}$$

The diaphragm rupture force was approximated as follows

— up to the moment of maximal power

$$R_0 = A_q\{\exp[B_q(X_1 - X_0)] - 1\}$$

— from the moment of maximal power to the diaphragm rupture

$$RP = D(4)X_0^4 + D(3)X_0^3 + D(2)X_0^2 + D(1)X_0 + D(0) \tag{2.2}$$

The pusher plate friction force was approximated to the form

$$T_{n-1} = E(4)X_{n-1}^4 + E(3)X_{n-1}^3 + E(2)X_{n-1}^2 + E(1)X_{n-1} + E(0) \tag{2.3}$$

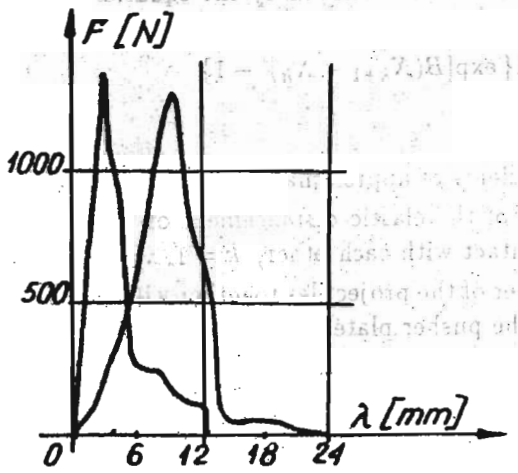

Fig. 18. Rupture of two diaphragms versus their deformation

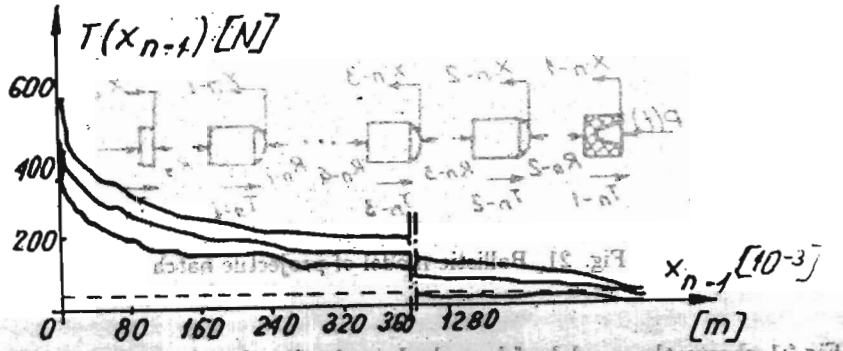

Fig. 19. Pusher plate friction versus its travel distance

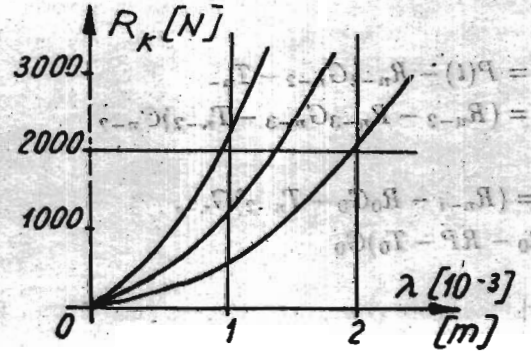

Fig. 20. Elastic deformation of a projectile – R_k force diagram

The elasticity force of projectiles can be described by the equation

$$R_k = A\{\exp[B(X_{k+1} - X_k)] - 1\} \tag{2.4}$$

where

A, A_q, B, B_q... – coefficients of approximation,

$X_{k+1} - X_k$ – value of the elastic displacement of projectiles being in contact with each other, $k = 1, ..., n-2$

n – number of the projectiles together with the diaphragm and the pusher plate.

3. Equations of projectiles movement

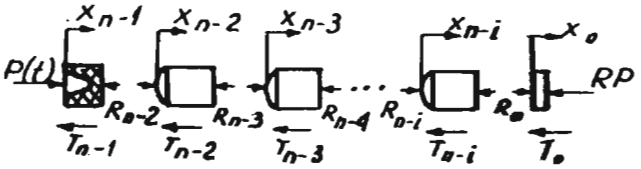

Fig. 21. Ballistic model of projectile batch

Fig.21 shows the model of launched projectiles batch applied to formulation of the projectiles movement equations (3.1). They have been derived according to d'Alembert's principle

$$\begin{aligned}
&m_{n-1}\ddot{X}_{n-1} = P(t) - R_{n-2}G_{n-2} - T_{n-1}\\
&m_{n-2}\ddot{X}_{n-2} = (R_{n-2} - R_{n-3}G_{n-3} - T_{n-2})G_{n-2}\\
&\dots\\
&m_{n-i}\ddot{X}_{n-i} = (R_{n-i} - R_0G_0 - T_{n-2})G_{n-i}\\
&m_0\ddot{X}_0 = (R_0 - RP - T_0)G_0
\end{aligned} \tag{3.1}$$

where

$i = n - 1$

$\ddot{X} = d^2X/dt^2$

$p(t)$ – force causing the pusher plate movement,
T – force of friction caused by tube walls,
R – force of elastic interactions between projectiles,
m – mass of projectiles,
S – cross-sectional area of the tube,
G – parameter which during computations equals 1 but when a projectile bottom reaches the tube outlet it equals 0.

The forces of elastic interactions may be neglected when the projectiles are not n contact with each other and when the bottom of a departing projectile reaches he outlet edge of the tube. In the second case the number of equations will be educed as $G = 0$.

4. Numerical computations

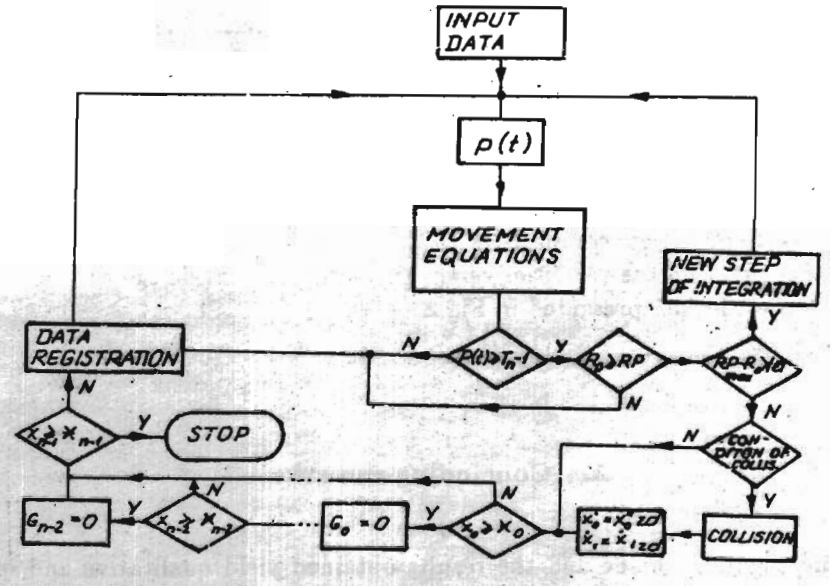

Fig. 22. Algorithm of numerical computations of launch for the tube launcher locked by a diagram

Computations were made in accordance to an algorithm shown in Fig.22. It as derived with application of the impact theory [5] related to collision of the first rojectile with the diaphragm when the force R_0 exceeded the value of RP_{max}

(Eq (2.2)). Application of the impact theory yields a good correlation in the diaphragm rupture characteristics computations.

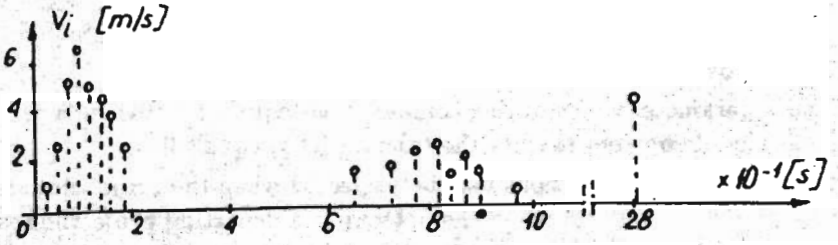

Fig. 23. Projectile departing times and the muzzle velocities corresponding with them obtained by numerical calculation

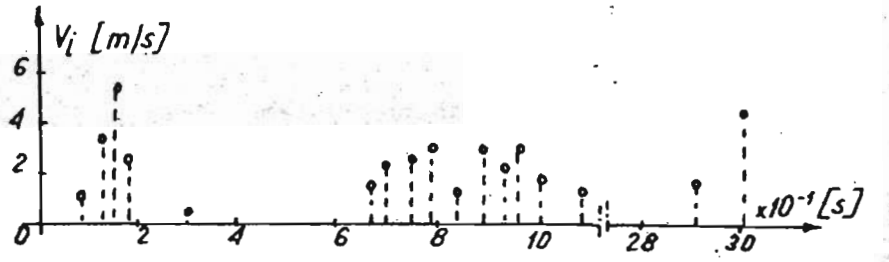

Fig. 24. Projectile departing times and the muzzle velocities corresponding with them obtained by experiment

Computations were made in the case of seventeen projectiles. Computed muzzle velocities (Fig.23) were compared with the experimental ones (see Fig.24). The forces of elasticity and the velocities versus throwing time inside the tube launcher for some projectiles are presented in Fig.25 ÷ 28.

5. Concluding remarks

The invesigations made and the results obtained yield qualitative and quantitative information which can be applied to the theoretical models design of the internal ballistics of the multiprojectile launchers.

One of the most important conclusions is the fact that the nature of projectile batch travel is predominantly determined by the elasticity forces between projectiles. Due to these interactions and the tube muzzle locking by the diaphragm the projectiles leave the tube at an irregular time intervals with different velocities.

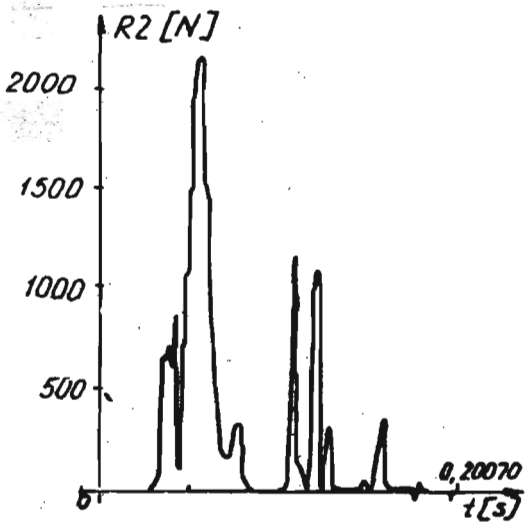

Fig. 25. Elasticity force acting on the 2nd projectile versus launch time

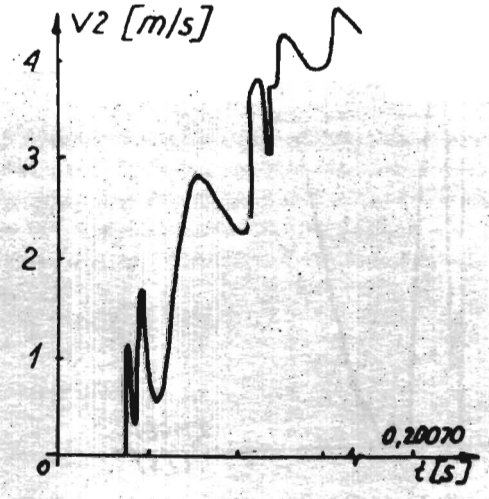

Fig. 26. Velocity of the 2nd projectile versus launch time

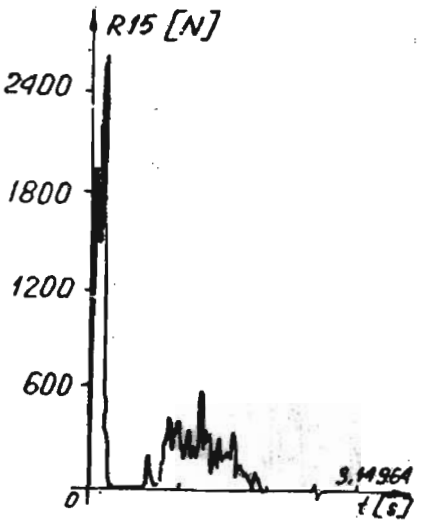

Fig. 27. Elasticity force acting on the 15th projectile versus launch duration time

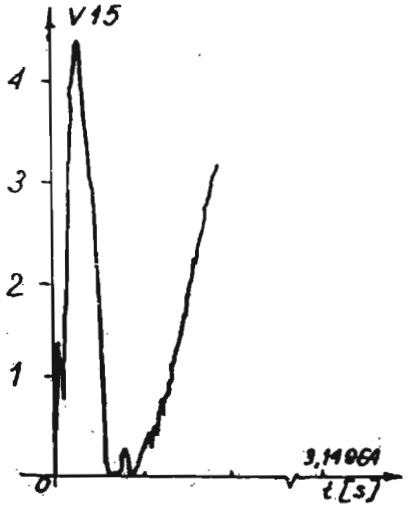

Fig. 28. Velocity of the 15th projectile versus launch duration time

References

1. KOŁOMAŃSKI K., 1983, *Miny i zapory minowe*, Wojskowy Przegląd Techniczny nr 10, Warszawa
2. GARSTKA J., 1990, *Minowanie narzutowe*, Wojskowy Przegląd Techniczny nr 1, Warszzawa
3. DUWALIAN S., 1967, *Issledowanie prodolnoj dinamiki pojezda na ECM*, Westnik WNIZT nr 7
4. GRZESIKIEWICZ W., 1975, *Badania na modelu matematycznym zjawisk dynamicznych występujących wzdłuż pociągu towarowego ze sprzęgami samoczynnymi*, Politechnika Warszawska
5. GRYBOŚ R., 1972, *Teoria uderzenia w dyskretnych układach mechanicznych*, PWN Warszawa
6. KROMKA J., 1989, *Badanie zjawisk zachodzących w wielopociskowej wyrzutni rurowej podczas miotania*, Informator Instytutu Technicznego Wojsk Lotniczych nr 71, Warszawa
7. KROMKA J., 1990, *Badania balistyczne wielopociskowego układu miotającego*, Wojskowa Akademia Techniczna, Warszawa

6. Szeregowy układ miotający pakiet pocisków sprężystych z zamkniętej przeponą wyrzutni rurowej

Streszczenie

W artykule przedstawiono metody i wyniki badań wielopociskowej wyrzutni rurowej. Podczas badań określono przemieszczanie się kolejnych pocisków wzdłuż wyrzutni i wykonano pomiary ciśnienia w przestrzeni zatłokowej.

Do opisu miotania konieczne były badania uzupełniające podczas których wyznaczono siłę tarcia tłoka i pocisków, siłę sprężystości pocisków oraz siłę zrywania przepony. Zmierzone siły i ciśnienia aproksymowano do postaci funkcji matematycznych. Model miotania pakietu pocisków, których przemieszczenie jest powodowane działaniem siły ciśnienia pochodzącego ze spalania ładunku pirotechnicznego, poddano obliczeniom numerycznym. Porównano wyniki obliczeń prędkości wylotowych pocisków z wynikami otrzymanymi z eksperymentu.

Manuscript received October 10, 1991; accepted for print March 25, 1992